HHS Public Access

Author manuscript

Cell Rep. Author manuscript; available in PMC 2020 December 01.

Published in final edited form as:

Cell Rep. 2020 October 27; 33(4): 108316. doi:10.1016/j.celrep.2020.108316.

Lysosomal Acid Lipase Is Required for Donor T Cells to Induce Graft-versus-Host Disease

Hung D. Nguyen[1,6,7], **Taylor Ticer**[1,6], **David Bastian**[1,6], **Sandeepkumar Kuril**[2], **Hong Li**[3], **Hong Du**[4], **Cong Yan**[4], **Xue-Zhong Yu**[1,5,8,*]

[1]Department of Microbiology and Immunology, Medical University of South Carolina, Charleston, SC 29425, USA

[2]Department of Pediatric Hematology-Oncology, Medical University of South Carolina, Charleston SC 29425, USA

[3]Department of Public Health, Medical University of South Carolina, Charleston, SC 29425, USA

[4]Department of Pathology and Laboratory Medicine, Indiana University School of Medicine, Indianapolis, Indianapolis, IN 46202, USA

[5]Department of Medicine, Medical University of South Carolina, Charleston, SC 29425, USA

[6]These authors contributed equally

[7]Present address: College of Medicine, University of Central Florida, Orlando, FL 32827, USA

[8]Lead Contact

SUMMARY

Graft-versus-host disease (GVHD) limits the success of allogeneic hematopoietic cell transplantation (allo-HCT). Lysosomal acid lipase (LAL) mediates the intrinsic lipolysis of cells to generate free fatty acids (FFAs), which play an essential role in the development, proliferation, and function of T cells. Here, we find that LAL is essential for donor T cells to induce GVHD in murine models of allo-HCT. Specifically, LAL is required for donor T cell survival, differentiation, and alloreactivity in GVHD target organs, but not in lymphoid organs. LAL induces the differentiation of donor T cells toward GVHD pathogenic Th1/Tc1 and Th17 while suppressing regulatory T cell generation. $LAL^{-/-}$ T cells succumb to oxidative stress and become anergic in target organs. Pharmacologically targeting LAL effectively prevents GVHD development while preserving the GVL activity. Thus, the present study reveals the role of LAL in

*Correspondence: yux@musc.edu.

AUTHOR CONTRIBUTIONS

H.D.N. and X.-Z.Y. designed the study; H.D.N., T.T., D.B., and S.K. conducted experiments and participated in acquiring and analyzing data; H.D.N., T.T., and X.-Z.Y. interpreted the data and wrote the manuscript; C.Y. and H.D. provided the genetic knockout (KO) mice. H.D.N., T.T., D.B., S.K., C.Y., H.D., and X.-Z.Y. participated in editing the manuscript.

SUPPLEMENTAL INFORMATION

Supplemental Information can be found online at https://doi.org/10.1016/j.celrep.2020.108316.

DECLARATION OF INTERESTS

The authors declare no competing interests.

T cell alloresponse and pathogenicity and validates LAL as a target for controlling GVHD and tumor relapse after allo-HCT.

Graphical Abstract

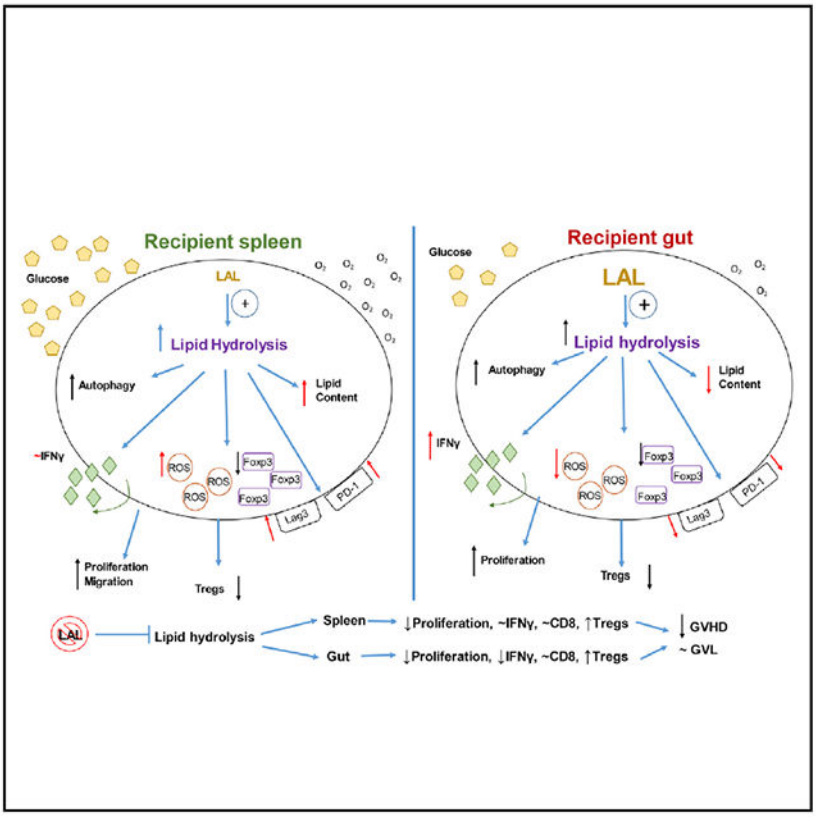

In Brief

Nguyen et al. demonstrate that LAL regulates T cell activity in GVHD target and lymphoid organs differentially. Blocking LAL preferentially reduces the activation and proliferation of CD4, spares CD8, promotes regulatory T cells, and diminishes T cell migration to and activation in the recipient gut, thus alleviating GVHD while maintaining GVL activity.

INTRODUCTION

Graft-versus-host disease (GVHD) limits the success of allogeneic hematopoietic cell transplantation (allo-HCT) (Ferrara et al., 2009). Cell metabolism determines T cell fate and function by regulating nutrition intake and transcription factor expression (Buck et al., 2015). The metabolic characteristics of pathogenic T cells are different in various immunological diseases such as rheumatoid arthritis (RA), systemic lupus erythematosus (SLE), and colitis (Biniecka et al., 2011; Gerriets et al., 2014; Wahl et al., 2010; Yang et al., 2013). Among these diseases, colitis shares many immunological similarities with gut GVHD, which is the most common GVHD target organ, potentially leading to life-threatening complications (Naymagon et al., 2017).

Fatty acid (FA) metabolism has been implicated in GVHD development after allo-HCT. A study by Gatza et al. (2011) demonstrated that the oxidation of FAs (FAO) in mitochondria is responsible for the generation of alloreactive T cells, which are the driving force in GVHD. Therefore, blocking FAO via targeting mitochondrial F(1)F(0) adenosine triphosphate synthase (F(1)F(0)-ATPase) or Cpt1a (the enzyme responsible for FA uptake into mitochondria) (Byersdorfer et al., 2013) induces the apoptosis of alloreactive T cells. However, no attempt has been made to block the resources of cytosolic FAs for tricarboxylic acid (TCA)-dependent FAO in mitochondria to control GVHD.

Lipolysis of stored lipids generates FAs that can be used as energy substrates through FAO in the TCA cycle (Zechner et al., 2012). Several enzymes regulate the release of FAs from lipid droplets under changing nutrition state. Lysosomal acid lipase (LAL) is an intracellular lipase that catalyzes the hydrolysis of cholesteryl esters and triglycerides in lysosomes at acidic pH (Qu et al., 2009). LAL plays a central role in lipid metabolism in lymphocytes and is required for the normal development, maturation, and functionality of this type of cell (Qu et al., 2009). In addition, in the absence of LAL, T cell receptor (TCR) activation, T cell proliferation, and cytokine secretion are tremendously impaired (Schlager et al., 2017). LAL supports the metabolic reprogramming necessary for CD8 memory ($CD8_{mem}$) development (O'Sullivan et al., 2014). However, how LAL regulates alloreactive T cell metabolism, survival, activation, and GVHD pathogenesis has not been studied. Recently, LAL has been shown to affect T cell differentiation, as CD4 T cells deficient for LAL have a reduced ability to differentiate into T helper 1 and 2 (Th1/Th2) cells while increasing the generation of regulatory T cells (Tregs) (Qu et al., 2009). Because Th1 cells are pathogenic and Tregs are suppressive in GVHD (Nguyen et al., 2018b), LAL targeting may be beneficial for controlling GVHD.

In the present study, we found that LAL was required for donor T cells to induce GVHD after allo-HCT. LAL-deficient T cells retained sufficient anti-tumor activity to prevent tumor relapse. The pharmacological blockade of LAL effectively prevented or treated GVHD while maintaining the graft versus leukemia (GVL) effect. Our study therefore validated LAL in T cells as a potential target for controlling GVHD and tumor relapse after allo-HCT. Given that LAL-specific inhibitors have been traditionally used for the prevention or treatment of obesity in clinics, the outcome of this study is of high translational potential.

RESULTS

Hydrolysis of Lipid Affects T Cell Responses

FAs serve not only as fuel for cells but also as components of cell membrane phospholipids and glycolipids. In our previously published work, we found that donor T cells accumulated long-chain FAs in allogeneic recipients, which likely resulted from a decline in FAO and an increase in lipid hydrolysis (Nguyen et al., 2016). Among other enzymes, lysosomal acid lipase (LAL) is an important lipase responsible for hydrolyzing lipids in the droplets to free FAs and lysolipids during stress conditions (Gomaraschi et al., 2019; Rader, 2015). Unlike regulatory or memory T cells, effector T cells are known to require appreciable amounts of extracellular-free FA (Nguyen et al., 2018b; Tijaro-Ovalle et al., 2019). Furthermore, LAL was found to play a critical role in T cell development and function, while being dispensable

for Tregs (Qu et al., 2009). We therefore hypothesized that LAL is essential for T cell pathogenicity in the induction of GVHD. To test this hypothesis, we used LAL-deficient mice ($LAL^{-/-}$) as donors in allogeneic bone marrow transplantation (allo-BMT). Although T cell development in the thymus was partially impaired in the absence of LAL (Qu et al., 2009), we verified that immune phenotypes, including percentages of T cells, B cells, monocytes, and multiple T cell subsets (memory and regulatory), were comparable in peripheral lymphoid organs of young mice, regardless of LAL expression (data not shown). We next examined the effect of LAL on T cell survival, proliferation, and activation under polyclonal activation by CD3/CD28 *in vitro*. Upon stimulation, LAL-deficient T cells (both CD4 and CD8) exhibited increased necrosis (higher percentage of $7AAD^{+}$annexin V^{+}) (Figures 1A and 1C), decreased proliferation (lower percentage of carboxyfluorescein diacetate succinimidyl ester [CFSE] diluted) (Figures 1B and 1D), lower levels of pro-inflammatory cytokine production (interferon γ [IFN-γ] and tumor necrosis factor a [TNF-α]) (Figures 1E and 1G), and decreased FA oxidation (lower percentage of peroxisome proliferator-activated receptor gamma, $PPR\gamma^{+}$) (Figures 1F and 1H), as compared to wild-type (WT) counterparts.

To understand the role of LAL in alloantigen-induced T cell response, we performed an *in vitro* mixed lymphocyte reaction (MLR) assay in which CFSE-labeled bulk T cells from $LAL^{+/+}$ and $LAL^{-/-}$ FVB mice were stimulated with T cell-depleted (TCD) splenocytes from BALB/c mice. Consistent with polyclonal stimulation, $LAL^{-/-}$ $CD4^{+}$ T cells had less cell survival, reduced proliferation reflected by lower Ki67 expression and CFSE, and reduced activation reflected by low levels of IFN-γ production as compared to WT T cells (Figures S1A and S1B). Under this condition, $LAL^{-/-}$ $CD4^{+}$ T cells also exhibited lower lipid content, FAO, reactive oxidative species (ROS) formation, and co-inhibitory molecules, which were reflected by BODIPY uptake, Cpt1a expression, 2′,7′-dichlorofluorescin diacetate (DCFDA) intensity, and programmed cell death-1 (PD-1)/Lag3 expression, respectively (Figure S1C). We interpret that these reductions resulted from lower T cell activation in the absence of LAL. Similar trends were observed on $LAL^{-/-}$ $CD8^{+}$ T cells, although the levels of compromise were less profound (data not shown).

The dysfunction of $LAL^{-/-}$ $CD4^{+}$ T cell responses may be due to reduced survival in culture. To test the hypothesis, we stimulated LAL $^{+/+}$ and $LAL^{-/-}$ T cells with allogenic antigen-presenting cells (APCs) as in Figure S1, but also supplemented N-acetyl cysteine (NAC), a known antioxidant. We found that additional NAC significantly reduced proliferation, IFN-γ production and PD-1 expression of $LAL^{+/+}$, but not $LAL^{-/-}$ T cells (Figure S2). These results are consistent with higher ROS generation by $LAL^{+/+}$ T cells, and suggest that inferior survival may not be the reason for T cell dysfunction in the absence of LAL. The dysfunction of $LAL^{-/-}$ $CD4^{+}$ T cell responses may be due to impaired lipid metabolism. To test this hypothesis, we used media containing lipid-free serum (LF). Interestingly, while LF media reduced the proliferation and activation of $LAL^{+/+}$ T cells, it increased the proliferation and activation of $LAL^{-/-}$ T cells (Figures S2A and S2B). These results indicate that external lipids facilitate optional T cell activation, but LAL dictates its contribution to T cell response.

LAL$^{-/-}$ T Cells Have Reduced Capacity to Induce GVHD

Because T cell survival and activation are required for donor T cells to induce GVHD, we hypothesized that targeting LAL in donor T cells would alleviate GVHD severity. Using major histocompatibility complex (MHC)-mismatched B6 (H2^{b}) → BALB/c (H2^{d}) and FVB (H2^{q})→B6 (H2^{b}) BMT models, we found that LAL-deficient donor T cells induced significantly less severe GVHD compared with WT control T cells, which is reflected by recipient survival and clinical scores (Figures 2A–2D). Because the primary purpose of allo-HCT is to eradicate hematological malignance (Bleakley and Riddell, 2004), we asked whether LAL-deficient T cells still retained sufficient activity to mediate the GVL response. Using luciferase-transduced P815 mastocytoma in the haploidentical B6 (H2^{b})→BDF1 (H2$^{b/d}$) BMT model, we observed that all of the recipients transplanted with T cell-depleted bone marrow cells (TCD-BMs) plus P815 died of tumor relapse, as indicated by strong luminescent signals (Figures 2E and 2G). The recipients with additional LAL$^{+/+}$ T cells all died within 20 days after BMT without tumor signal and significant GVHD severity (Figures 2E–2G), indicating that they died from GVHD, not tumor relapse. In contrast, 50% of the recipients with additional LAL$^{-/-}$ T cells survived without GVHD clinical signs until day 60 after transplant, and the majority of them were tumor free (Figures 2E and 2G). These data suggest that LAL is essential in donor T cells to induce GVHD, while it is dispensable for the GVL effect.

Pharmacological Inhibition of LAL Effectively Controls GVHD While Preserving the GVL Effect

For translational purposes, we tested the LAL-specific inhibitor of LAL orlistat (Huang et al., 2014) on the T cell alloresponse. Similar to LAL deficiency, we found that orlistat significantly inhibited proliferation, activation, and FA metabolism of CD4 and CD8 T cells, as reflected by Ki67 expression, IFN-γ production, and Cpt1a expression, respectively (Figures S3A–S3D). It is worth noting that orlistat treatment also increased Foxp3 expression on CD4 T cells, although not as profoundly as in the absence of LAL (Figure S3C). These results demonstrate that LAL can be targeted pharmacologically through orlistat.

We next assessed the effect of orlistat GVH and GVL responses. By titrating the doses, orlistat was found to be not toxic when administrated to BMT recipients at 8–20 mg/kg/day for 14 days (Figure 3A). Treatment with orlistat effectively prevented GVHD development in recipients, indicated by the improvement of survival and lower clinical scores (Figures 3A and 3B). To investigate the effect of orlistat on the GVL activity against leukemia and lymphoma, we used two GVHD/GVL models. In the B6 to BDF1 model with P815 leukemia, all of the recipients with BM alone died from tumor relapse, reflected by heavy tumor signals before death (Figures 3C–3E). The recipients transplanted with donor T cells and treated with vehicle died from GVHD with little tumor signal (Figure 3E). However, orlistat treatment rescued 40% of the recipients from lethal GVHD and tumor relapse (Figures 3C–3E). To extend the observations to a different model, we used the B6 to BALB/c BMT model in combination with host-derived mixed-lineage leukemia (MLL-AF9). Orlistat treatment improved recipient survival and decreased GVHD clinical signs (Figures S4A and S4B). As expected, all of the recipients with BM alone died from tumor

relapse, reflected by MLL in peripheral blood but no GVHD clinical signs before death (Figure S4A–S4D). Orlistat treatment did not alter the outcomes of the recipients with BM alone, indicating that orlistat had little or no direct effect on leukemia growth. However, orlistat treatment maintained the GVL effect, as the recipients under orlistat treatment did not exhibit leukemia (Figures S4C and S4D). These results illustrate that pharmacologically targeting LAL may be an effective approach for the control of GVHD while sparing the GVL effect.

LAL Affects Donor T Cells Differentially in Lymphoid and Target Organs after Allo-HCT

To understand how LAL affects T cell immunity *in vivo,* we performed allo-BMT and analyzed donor T cells in recipient spleens (Figure 4) and guts (Figure 5) 7 days after transplant. Consistent with our observations *in vitro* (Figure S1), $LAL^{-/-}$ donor CD4 T cells significantly reduced proliferation (Ki67), migration potential (CXCR3), and intercellular lipid content (BODIPY), but increased Treg generation (Foxp3), compared to $LAL^{+/+}$ CD4 T cells in recipient spleens (Figures 4B, 4E–4G, and 4I). In contrast to CD4 T cells, the deficiency of LAL had little effect on donor CD8 T cells (Figures 4C–4J). The treatment of recipients with orlistat essentially phenocopied LAL deficiency, except for increasing Treg generation (Figure 4G). Unlike *in vitro* culture (Figure S1), neither LAL deficiency or orlistat treatment had a significant effect on ROS generation (DCFDA and PD-1 expression of donor T cells (Figures 4H and 4J).

As the gut is a main target organ in GVHD, we examined donor T cells in recipient intestines (Figure 5). Unlike in recipient spleens, donor $LAL^{-/-}$ T cells ($H2K^{d-}$), especially CD4, significantly decreased in recipient guts as compared to WT counterparts (Figures 5A and 5D). Given that Ki67 expression was comparable (data not shown), we interpret that reduced $LAL^{-/-}$ T cells in recipient guts were due to impaired survival and/or migration (Figures 5B, 5C, and 5F).

In sharp contrast to T cells in the spleen, both donor CD4 and CD8 T cells deficient for LAL in the gut had significantly increased intracellular lipid content reflected by BODIPY uptake (Figures 5B, 5C, and 5G), suggesting that T cells require LAL to hydrolyze lipid in the gut. Similarly, donor T cells deficient for LAL also had significantly increased ROS generation reflected by DCFDA intensity in recipient guts (Figures 5B, 5C, and 5H). However, an increase in the level of T cell exhaustion was seen, as reflected by PD-1 expression (Figure 5B, 5C, and 5I). Consistent with results observed in the spleen, Treg generation was also increased in $LAL^{-/-}$ CD4 T cells in the recipient gut (Figures 5B and 5E). By and large, the treatment of recipients with orlistat simulated LAL deficiency, with notable exceptions where orlistat treatment significantly decreased CXCR3 expression and failed to increase Foxp3 expression on donor T cells that differed from the effects of LAL deficiency (Figures 5E and 5F). We observed that LAL regulated T cell response differentially in lymphoid (spleen) and in target (gut) organs in the development of GVHD, which likely results from distinct microenvironments.

LAL Regulates T Cell Activation and Differentiation

At 7 days after BMT, we also examined the effects of LAL on cytokine production by donor T cells, but we did not find a major impact of LAL deficiency or orlistat treatment on IFNγ or IL-17 production either in recipient spleens or guts (data not shown). Given that GVHD severity was markedly reduced when targeting LAL either genetically or pharmacologically, we reasoned that the impact of LAL would be more profound later after BMT. We examined the effects of LAL deficiency in T cell activation, cytokine production, and metabolism in recipient spleens 13 days after BMT before the recipients of WT T cells. As shown in Figure S5A, the recipients of $LAL^{-/-}$ T cells had significantly lower clinical scores and body weight losses than those receiving $LAL^{+/+}$ T cells, confirming a reduced pathogenicity of $LAL^{-/-}$ T cells in the induction of GVHD. We measured mammalian target of rapamycin complex 1 (mTORC1) activity as it reflects T cell activation, and found it was comparable between $LAL^{-/-}$ and $LAL^{+/+}$ T cells, as demonstrated by the significantly increased density of phospho-S6 (pS6) in donor CD4 and CD8 T cells (Figure S5B). Interestingly, the mitochondrial membrane potential (Figure S5C), mitochondrial number (Figure S5F), and respiration (Figure S5G) were increased in $LAL^{-/-}$ T cells. The migration of donor lymphocytes toward GVHD target organs is required for GVHD development. Chemokine receptors expressed on the surface of lymphocytes is responsible for the trafficking of these cells toward target organs (Zeiser and Blazar, 2017). We found that $LAL^{-/-}$ CD4 T cells expressed lower gut/lung homing chemokine CXCR3 as compared to that of $LAL^{+/+}$ CD4 T cells in recipient spleens (Figures S5D and S5E). Cytokine production including IFNγ and IL-17 was not different between $LAL^{-/-}$ and $LAL^{+/+}$ T cells in recipient spleens (data not shown). These results indicate that $LAL^{-/-}$ T cells did not impair T cell activation and metabolism, but did reduce the T cell migration potential.

We next focused on examining the impact of LAL in T cells of the gut, a main GVHD target organ. Gut damage caused by conditioning, such as total body irradiation (TBI), triggers systemic GVHD development (Naymagon et al., 2017). Given that cell death is a valid indicator of gut damage (Jalili-Firoozinezhad et al., 2018), we isolated intestinal cells and examined their viability. Both percentage and absolute number of necrotic cells ($7\text{-AAD}^{+}\text{annexin V}^{+}$) among host non-hematopoietic cells were significantly lower in the recipients of $LAL^{-/-}$ T cells (Figures 6A and 6B), suggesting that $LAL^{-/-}$ T cells caused less gut damage. T cell differentiation into pathogenic phenotypes is critical for the development of GVHD. As LAL was previously to be involved in T cell differentiation (Qu et al., 2009), we assessed the impact of LAL in donor T cell differentiation *in vivo*. In recipient guts, LAL-deficient T cells exhibited reduced percentages of $\text{IFN-}\gamma^{+}$ and IL-17^{+} cells while increasing Foxp3^{+} cells (Figures 6C–6E), suggesting that LAL promotes Th1/Th17 cell differentiation while suppressing Treg generation. These data suggest that LAL regulates GVHD pathogenicity via modulating donor T cell activation, differentiation, and migration in the recipient gut.

LAL Effects on Donor T Cell Metabolism in GVHD Target Tissue

We next examined how LAL affects donor T cell fate in the recipient gut. We observed that donor T cells deficient for LAL exhibited significantly higher percentages of necrosis, reflected by 7-AAD^{+}/annexin V^{+} cells (Figure 7A) and lower levels of proliferation,

reflected by Ki67 expression (Figure 7B). Oxidative stress has been implicated in T cell death in GVHD target organs. Free FAs (FFAs) that are generated through lipid hydrolysis and subsequently undergo FAO in mitochondria reduce oxidative stress (Galicia-Vázquez and Aloyz, 2018). We therefore examined oxidative stress levels via DCFDA staining and found that donor CD4 T cells deficient for LAL showed higher levels of oxidative stress, reflected by higher levels of DCFDA uptake (Figure 7C). LAL deficiency likely caused lipid accumulation in donor T cells in recipient gut tissue as lipid content, reflected by BOD-IPY uptake, was increased in both donor CD4 and CD8 T cells (Figure 7D). In addition, cpt1a expression levels were significantly decreased in $LAL^{-/-}$ CD4 T cells, suggesting that FAO was decreased in the absence of LAL (Figure 7E). We also observed that exhaustion markers such as PD-1 and LAG-3 were significantly increased in $LAL^{-/-}$ T cells (Figures 7F and 7G). These data suggest that donor T cells in target organs are in a state of anergy/exhaustion in the absence of LAL. Autophagy is required for T cells to survive and maintain function in stressful conditions, such as GVHD target organ environment (Le Texier et al., 2016). We found that donor T cells decreased autophagy activity in the absence of LAL, reflected by Cyto-ID staining (Figure 7H). We also observed a trend of increase in PD-L1 expression in recipient non-hematopoietic stem cells ($CD45^{-}$) (Figure 7I). These results indicate that LAL is required for T cell survival, function, and proliferation in GVHD target organs.

DISCUSSION

In the present study, we used both genetic and pharmacological approaches to determine the involvement of lipid metabolism in GVHD pathogenicity (Byersdorfer et al., 2013; Nguyen et al., 2018b). How FA metabolism regulates T cell responses after allo-HCT is still controversial (Gatza et al., 2011; Nguyen et al., 2016). It is also not clear what resources of FAs are required for the energetic demand of allo-reactive T cells. By using genetic and pharmacological approaches, we demonstrated that LAL, which is responsible for the release of FAs from lipid droplets, is important in donor T cell survival, metabolism, and function. The present study provides rationale for targeting LAL for the control of GVHD and tumor relapse after allo-HCT.

LAL has been shown to play a critical role in TCA-dependent FAO in CD8 memory T cells (O'Sullivan et al., 2014). However, the role of LAL in CD4 T cell metabolism is still unclear, which is relevant in understanding the development of GVHD (Coghill et al., 2011). We observed that LAL was required for FAO, reflected by reduced PPRγ expression in proliferating T cells in the absence of LAL (Figures 1F and 1H). Donor T cells typically differentiate into pathogenic phenotypes such as Th1 and Th17 cells in GVHD pathobiology after allo-HCT (Shlomchik, 2007). Metabolic microenvironments are known to be different in secondary lymphoid and parenchymal tissues (Dumitru et al., 2018). We observed that LAL induces Th1/Tc1 and Th17 cell differentiation while suppressing Treg generation, specifically in GVHD target organs but not in lymphoid organs. This observation suggests that LAL affects T cell differentiation after activation by alloantigens and migration to target organs. It is possible that alloreactive T cells depend more on FAs released from lipid droplets to fulfill their energy demands under the hypoxia and nutritional stress conditions in target organs (Gupta et al., 2017). It has recently become apparent that CD4 T cells, in

response to the starvation and inflammation of microenvironments such as in the GVHD gut, use autophagy as a mechanism for survival (Li et al., 2006). While LAL is essential for autophagy initiation, the absence of LAL may lead to a reduced memory formation and increased anergy of T cells (Puleston et al., 2014). The level of autophagy was decreased in gut $LAL^{-/-}$ T cells, as shown in Figure 7H. By contrast, in lymphoid organs such as the spleen, where external nutrition (e.g., glucose, glutamine) and oxygen are widely available (Pearce et al., 2013), T cells may not depend on intracellular energy resources for survival and function. The level of intracellular FA in donor T cells was decreased in the spleen when LAL was absent or blocked (Figure 4I), and thus we observed a limited impact of LAL on T cell immunological phenotype in recipient spleens.

Another potential explanation is that under a hypoxia condition, alloreactive T cells depend more on glycolysis for their survival and function (Nguyen et al., 2016), which would increase the generation of lactate and then further activate LAL under an acidic microenvironment (Qu et al., 2010). Therefore, LAL may promote alloreactive T cell survival to cause more damage in parenchymal organs. In contrast, oxygen is abundant in lymphoid organs, as these organs are well interconnected with peripheral blood (Gupta et al., 2017). The absence of LAL may be compensated for by other metabolic pathways. In favor of this, in the absence of LAL, donor T cells increase the oxygen consumption rate (OCR), which is correlated with an increased in the total number of mitochondria in recipient lymphoid organs (Figure S5). The preserved survival and function of CD8 T cells in lymphoid organs in the absence of LAL likely contributed to the maintenance of the GVL effect.

It is well documented that PD-L1/PD-1 signaling plays an important role in the survival and metabolism of T cells in GVHD target organs (Ni et al., 2017). The coincidence of PD-L1 upregulation on non-hematopoietic cells and PD-1 upregulation on $LAL^{-/-}$ T cells in recipient guts (Figures 7F and 7I) suggests that PD-L1/PD-1 ligation may contribute to T cell anergy in the absence of LAL. The upregulation of PD-L1 in gut non-hematopoietic cells may result from the stress of GVHD development, where $LAL^{-/-}$ T cells compete with gut cells for essential nutrition such as FAs (Wangpaichitr et al., 2017). However, further studies are required to confirm this assumption.

Of importance, we have evaluated a translational approach and demonstrated that an LAL-specific inhibitor (orlistat) can effectively prevent GVHD, while still largely preserving the GVL activity of donor T cells. Although the inhibition of LAL in the recipients mimicked the results of LAL-deficient donor T cells, we cannot assume that orlistat merely inhibited LAL on T cells. In fact, the impact of orlistat on the generation of myeloid-derived suppressor cells (Schlager et al., 2017) and M2 macrophages (Huang et al., 2014) may also be attributed to overall outcomes, as suggested by others (Koehn and Blazar, 2017). In summary, the present study provides evidence that LAL may be a promising target for the control of GVHD and tumor relapse after allo-HCT. Because many lipase inhibitors are available or in clinical trials against obesity, the present findings have high translational potential in clinics.

STAR★METHODS

RESOURCE AVAILABILITY

Lead Contact—Further information or requests should be directed to Xue-Zhong Yu (yux@musc.edu).

Materials Availability—Requests for unique resources should be directed to the lead contact. A completed Materials Transfer Agreement may be required.

Data and Code Availability—The published article includes all datasets generated or analyzed in this study, including those in Figures S1–S5 in the PDF file attached. Original raw data are available from the corresponding author on request.

EXPERIMENTAL MODEL AND SUBJECT DETAILS

Animals and Chemicals—$LAL^{-/-}$ and $LAL^{+/+}$ strains on C57BL/6 (B6) or FVB backgrounds were established previously (Qu et al., 2009) and bred at the Medical University of South Carolina (MUSC). FVB (H-$2^{q,}$ CD45.1), C57BL/6 (H-2^{b}, CD45.2), B6 Ly5.1 (H-2^{b}, CD45.1), B6D2F1 (H-$2^{b/d}$, CD45.2), C3H-SW (H-2^{b}, CD45.1), and BALB/c (H-2^{d}) mice were purchased from the National Cancer Institute or Charles River lab. Donor mice were age (6-10 weeks) and gender (both male and female) matched for experiments. Recipient mice were females age 8-10 weeks. Animals were maintained in specific pathogen-free facilities in the American Association for Laboratory Animal Care-accredited Animal Resource Center at MUSC. All animal procedures were approved by the Institutional Animal Care and Use Committee of MUSC. Orlistat was purchased from Cayman Chem.

METHOD DETAILS

Mixed Lymphocyte Reaction (MLR) *in vitro*—CD25-depleted T cells were purified from the spleen and lymph nodes from $LAL^{+/+}$ or $LAL^{-/-}$ mice on FVB background using microbeads via negative selection (Miltenyi). Purified T cells were labeled with CFSE and stimulated at 1.5×10^5 per well with 4.5×10^5 T cell depleted (TCD) splenocytes from BALB/c mice. In some conditions, cells were cultured in the media supplemented with lipid-free FBS (Thermo Fisher Scientific). In other conditions, 10 mM N-acetyl cysteine (NAC, Sigma) or 100 ug/ml Orlistat was added in cell culture. Cells were harvested five days after stimulation and subjected to flow-cytometric assays.

GVHD/GVL models—Recipient mice were lethally irradiated at 700 cGy for BALB/c and 1000-1200 cGy (2 split doses, 3-hour interval) for B6 or BDF1 recipient mice using an X-RAD 320 irradiator (Precision X-Ray). Lethally irradiated BALB/c, B6 or BDF1 mice were transplanted with BM from B6 or FVB donors with or without T cells at doses indicated. Recipient survival was monitored throughout the experiment. The development of GVHD was monitored twice per week for weight loss and once per week for clinical signs of posture, skin damage, hair loss, ruffled fur, diarrhea, and decreased activity (Nguyen et al., 2018a)(Cooke etal., 1996). To evaluate the GVL response, tumor cells were injected *i.v.* on the same day of transplantation. In case of luciferase transduced P815 (5000 cells/mouse),

tumor burden was estimated with bioluminescent imaging (BLI) using Xenogen-IVIS 200 *in vivo* Imaging System (Perkin-Elmer, Waltham, MA). MLL-AF9-GFP$^+$ tumors were identified by measuring via the percentages of GFP$^+$ cells in peripheral blood using flow cytometry. Recipient survival and GVHD severity demonstrated by recipient weight loss were monitored throughout experiment.

Flow Cytometry—The following antibodies were used for cell-surface staining: anti–CD4 (clone RM4-5, BD Biosciences), anti–CD8 (clone 53-6.7, BD Biosciences), anti–H-2^q (KH114, Biolegend), anti–CXCR3-biotin (CXCR3-173, eBioscience); and anti–CCR6-AF647 (BioLegend, clone 29-2L17), anti-FasL (MFL3, BD Biosciences), anti-PD-1 (MFL3, eBioscience), anti-NK1.1 (PK136, eBioscience), anti-CD44 (IM7, Biolegend), anti-CD62L (MEL-14, eBioscience), anti-TCRβ (H57-597 BD Biosciences), anti-CD11b (M1/70, eBioscience). Biotinylated Abs were detected using APCcy7 (BD Biosciences, catalog 554063) or PEcy7 (BD Biosciences, catalog 557598) conjugated to streptavidin. To measure intracellular cytokines, cells were stimulated for 4–5 h at 37°C with PMA (100 ng/ml, Sigma-Aldrich) and ionomycin (500 ng/mL; Calbiochem, EMD) in the presence of GolgiStop (BD Biosciences). Fix and permeabilization were performed using Cytofix/Cytoperm Plus (BD Biosciences), followed by staining with the appropriate antibodies including anti–IFNγ (clone XMG1.2, eBioscience), anti–IL-17 (clone TC11-18H10.1, BioLegend), anti–IL-4 (clone 11B11, BD Biosciences), anti–IL-5 (clone TRFK5, eBioscience), anti–FOXP3, (clone FJK-16 s, eBioscience), anti-Ki67 (16A8, Biolegend), and anti–pS6-AF467 (Cell Signaling Technology, clone D57.2.2E). Live/dead yellow cell staining kit (catalog L-34968) and CFSE (catalog C1157) were purchased from Invitrogen. Apoptosis was measured by Annexin V kit (BD Biosciences, San Jose, CA).

Immunofluorescence staining—Splenic T cells were stained directly with MitoTracker Red (MTR, 1 mM) (Molecular Probes) in PBS (pH 7.4). DAPI (Vector Labs) was used for nuclear stains. Super-resolution imaging was performed using a Zeiss LSM 880 confocal microscope (Zeiss. Uniform field sizes of 240x240x40 μm dimensions were imaged with a 63x oil objective.

Metabolic assays—The metabolic profile of single-cell suspensions was determined using a Seahorse XF96 Analyzer (Seahorse Biosciences, Billerica, MA), as described in our previous work (Ref #30). Briefly, T cells (0.5-1.0x10^6/well) were attached to tissue culture plates for 30 minutes using Cell-Tak (BD, 354240)(Capasso et al., 2010). OCR were analyzed in response to 1.0 μM oligomycin, 1.0 μM fluoro-carbonyl cyanide phenylhydrazone (FCCP) and 2μM rotenone (Seahorse Bioscience) plus 100 nM antimycin A (Sigma-Aldrich). ECAR were measured under basal conditions, and following injection of three pharmacologic compounds; glucose (5.5 mM), oligomycin (1.0 μM), 2-DG (100 mM) (Everts et al., 2012).

QUANTIFICATION AND STATISTICAL ANALYSIS

Statistics—Data were analyzed using Prism GraphPad (version 7). Briefly, comparisons (e.g., clinical scores and body weight loss scores) between two groups were estimated using a nonparametric Mann-Whitney *U* test. The log-rank (Mantel-Cox) test was utilized to

compare the overall survival rates between groups. Statistical analysis of metabolism data was performed by Wilcoxon's rank sum tests for two-group comparisons and/or Kruskal–Wallis test for multiple-group (> 2) comparisons followed by the Dunnett's test. A *p*-value less than 0.05 is considered significant.

Supplementary Material

Refer to Web version on PubMed Central for supplementary material.

ACKNOWLEDGMENTS

This work is supported by NIH (National Institutes of Health, United States) grants R01 HL137373 and R01 HL140953 and the SmartState Endowment in Cancer Stem Cell Biology & Therapy Program (to X.-Z.Y.). Institutional resources at the Medical University of South Carolina were supported by NIH grants C06 RR15455 and P30 CA138313 (to Hollings Cancer Center).

REFERENCES

Biniecka M, Fox E, Gao W, Ng CT, Veale DJ, Fearon U, and O'Sullivan J (2011). Hypoxia induces mitochondrial mutagenesis and dysfunction in inflammatory arthritis. Arthritis Rheum. 63, 2172–2182. [PubMed: 21484771]

Bleakley M, and Riddell SR (2004). Molecules and mechanisms of the graft-versus-leukaemia effect. Nat. Rev. Cancer 4, 371–380. [PubMed: 15122208]

Buck MD, O'Sullivan D, and Pearce EL (2015). T cell metabolism drives immunity. J. Exp. Med. 212, 1345–1360. [PubMed: 26261266]

Byersdorfer CA, Tkachev V, Opipari AW, Goodell S, Swanson J, Sandquist S, Glick GD, and Ferrara JL (2013). Effector T cells require fatty acid metabolism during murine graft-versus-host disease. Blood 122, 3230–3237. [PubMed: 24046012]

Capasso M, Bhamrah MK, Henley T, Boyd RS, Langlais C, Cain K, Dinsdale D, Pulford K, Khan M, Musset B, et al. (2010). HVCN1 modulates BCR signal strength via regulation of BCR-dependent generation of reactive oxygen species. Nat. Immunol. 11, 265–272. [PubMed: 20139987]

Coghill JM, Sarantopoulos S, Moran TP, Murphy WJ, Blazar BR, and Serody JS (2011). Effector CD4+ T cells, the cytokines they generate, and GVHD: something old and something new. Blood 117, 3268–3276. [PubMed: 21245483]

Cooke KR, Kobzik L, Martin TR, Brewer J, Delmonte J Jr., Crawford JM, and Ferrara JL (1996). An experimental model of idiopathic pneumonia syndrome after bone marrow transplantation: I. The roles of minor H antigens and endotoxin. Blood 33, 3230–3239.

Dumitru C, Kabat AM, and Maloy KJ (2018). Metabolic Adaptations of $CD4^+$ T Cells in Inflammatory Disease. Front. Immunol. 9, 540. [PubMed: 29599783]

Everts B, Amiel E, van der Windt GJ, Freitas TC, Chott R, Yarasheski KE, Pearce EL, and Pearce EJ (2012). Commitment to glycolysis sustains survival of NO-producing inflammatory dendritic cells. Blood 120,1422–1431. [PubMed: 22786879]

Ferrara JL, Levine JE, Reddy P, and Holler E (2009). Graft-versus-host disease. Lancet 373, 1550–1561. [PubMed: 19282026]

Galicia-Vázquez G, and Aloyz R (2018). Ibrutinib Resistance Is Reduced by an Inhibitor of Fatty Acid Oxidation in Primary CLL Lymphocytes. Front. Oncol. 3, 411.

Gatza E, Wahl DR, Opipari AW, Sundberg TB, Reddy P, Liu C, Glick GD, and Ferrara JL (2011). Manipulating the bioenergetics of alloreactive T cells causes their selective apoptosis and arrests graft-versus-host disease. Sci. Transl. Med. 3, 67ra8.

Gerriets VA, Kishton RJ, Nichols AG, Macintyre AN, Inoue M, Ilkayeva O, Winter PS, Liu X, Priyadharshini B, Slawinska ME, et al. (2014). Metabolic programming and PDHK1 control CD4+ T cell subsets and inflammation. J. Clin. Invest. 125, 194–207. [PubMed: 25437876]

Gomaraschi M, Bonacina F, and Norata GD (2019). Lysosomal Acid Lipase: From Cellular Lipid Handler to Immunometabolic Target. Trends Pharmacol. Sci. 40, 104–115. [PubMed: 30665623]

Gupta S, Roy A, and Dwarakanath BS (2017). Metabolic Cooperation and Competition in the Tumor Microenvironment: Implications for Therapy. Front. Oncol. 7, 68. [PubMed: 28447025]

Huang SC, Everts B, Ivanova Y, O'Sullivan D, Nascimento M, Smith AM, Beatty W, Love-Gregory L, Lam WY, O'Neill CM, et al. (2014). Cell-intrinsic lysosomal lipolysis is essential for alternative activation of macrophages. Nat. Immunol. 15, 846–855. [PubMed: 25086775]

Jalili-Firoozinezhad S, Prantil-Baun R, Jiang A, Potla R, Mammoto T, Weaver JC, Ferrante TC, Kim HJ, Cabral JMS, Levy O, and Ingber DE (2018). Modeling radiation injury-induced cell death and countermeasure drug responses in a human Gut-on-a-Chip. Cell Death Dis. 9, 223. [PubMed: 29445080]

Koehn BH, and Blazar BR (2017). Role of myeloid-derived suppressor cells in allogeneic hematopoietic cell transplantation. J. Leukoc. Biol. 102,335–341. [PubMed: 28148718]

Le Texier L, Lineburg KE, Cao B, McDonald-Hyman C, Leveque-El Mouttie L, Nicholls J, Melino M, Nalkurthi BC, Alexander KA, Teal B, et al. (2016). Autophagy-dependent regulatory T cells are critical for the control of graft-versus-host disease. JCI Insight 1, e86850. [PubMed: 27699243]

Li C, Capan E, Zhao Y, Zhao J, Stolz D, Watkins SC, Jin S, and Lu B (2006). Autophagy is induced in CD4+ T cells and important for the growth factor-withdrawal cell death. J. Immunol. 177, 5163–5168. [PubMed: 17015701]

Naymagon S, Naymagon L, Wong SY, Ko HM, Renteria A, Levine J, Colombel JF, and Ferrara J (2017). Acute graft-versus-host disease of the gut: considerations for the gastroenterologist. Nat. Rev. Gastroenterol. Hepatol. 14,711–726. [PubMed: 28951581]

Nguyen HD, Chatterjee S, Haarberg KM, Wu Y, Bastian D, Heinrichs J, Fu J, Daenthanasanmak A, Schutt S, Shrestha S, et al. (2016). Metabolic reprogramming of alloantigen-activated T cells after hematopoietic cell transplantation. J. Clin. Invest. 126, 1337–1352. [PubMed: 26950421]

Nguyen H, Kuril S, Bastian D, Kim J, Zhang M, Vaena SG, Dany M, Dai M, Heinrichs JL, Daenthanasanmak A, et al. (2018a). Complement C3a and C5a receptors promote GVHD by suppressing mitophagy in recipient dendritic cells. JCI Insight 3, e121697.

Nguyen HD, Kuril S, Bastian D, and Yu XZ (2018b). T-Cell Metabolism in Hematopoietic Cell Transplantation. Front. Immunol. 9, 176. [PubMed: 29479351]

Ni X, Song Q, Cassady K, Deng R, Jin H, Zhang M, Dong H, Forman S, Martin PJ, Chen YZ, et al. (2017). PD-L1 interacts with CD80 to regulate graft-versus-leukemia activity of donor CD8+ T cells. J. Clin. Invest. 127,1960–1977. [PubMed: 28414296]

O'Sullivan D, van der Windt GJ, Huang SC, Curtis JD, Chang CH, Buck MD, Qiu J, Smith AM, Lam WY, DiPlato LM, et al. (2014). Memory CD8(+) T cells use cell-intrinsic lipolysis to support the metabolic programming necessary for development. Immunity 41, 75–88. [PubMed: 25001241]

Pearce EL, Poffenberger MC, Chang CH, and Jones RG (2013). Fueling immunity: insights into metabolism and lymphocyte function. Science 342, 1242454. [PubMed: 24115444]

Puleston DJ, Zhang H, Powell TJ, Lipina E, Sims S, Panse I, Watson AS, Cerundolo V, Townsend AR, Klenerman P, and Simon AK (2014). Autophagy is a critical regulator of memory CD8(+) T cell formation. eLife 3, e03706.

Qu P, Du H, Wilkes DS, and Yan C (2009). Critical roles of lysosomal acid lipase in T cell development and function. Am. J. Pathol. 174, 944–956. [PubMed: 19179613]

Qu P, Shelley WC, Yoder MC, Wu L, Du H, and Yan C (2010). Critical roles of lysosomal acid lipase in myelopoiesis. Am. J. Pathol 176, 2394–2404. [PubMed: 20348241]

Rader DJ (2015). Lysosomal Acid Lipase Deficiency-A New Therapy for a Genetic Lipid Disease. N. Engl. J. Med. 373, 1071–1073. [PubMed: 26352819]

Schlager S, Vujic N, Korbelius M, Duta-Mare M, Dorow J, Leopold C, Rainer S, Wegscheider M, Reicher H, Ceglarek U, et al. (2017). Lysosomal lipid hydrolysis providessubstratesforlipid mediatorsynthesis in murine macrophages. Oncotarget 8, 40037–40051. [PubMed: 28402950]

Shlomchik WD (2007). Graft-versus-host disease. Nat. Rev. Immunol. 7, 340–352. [PubMed: 17438575]

Tijaro-Ovalle NM, Karantanos T, Wang HT, and Boussiotis VA (2019). Metabolic Targets for Improvement of Allogeneic Hematopoietic Stem Cell Transplantation and Graft-vs.-Host Disease. Front. Immunol. 10, 295. [PubMed: 30891031]

Wahl DR, Petersen B, Warner R, Richardson BC, Glick GD, and Opipari AW (2010). Characterization of the metabolic phenotype of chronically activated lymphocytes. Lupus 19, 1492–1501. [PubMed: 20647250]

Wangpaichitr M, Kandemir H, Li YY, Wu C, Nguyen D, Feun LG, Kuo MT, and Savaraj N (2017). Relationship of Metabolic Alterations and PD-L1 Expression in Cisplatin Resistant Lung Cancer. Cell Dev. Biol. 6, 183. [PubMed: 28819582]

Yang Z, Fujii H, Mohan SV, Goronzy JJ, and Weyand CM (2013). Phosphofructokinase deficiency impairs ATP generation, autophagy, and redox balance in rheumatoid arthritis T cells. J. Exp. Med. 210, 2119–2134. [PubMed: 24043759]

Zechner R, Zimmermann R, Eichmann TO, Kohlwein SD, Haemmerle G, Lass A, and Madeo F (2012). FAT SIGNALS-lipases and lipolysis in lipid metabolism and signaling. Cell Metab. 15, 279–291. [PubMed: 22405066]

Zeiser R,and Blazar BR(2017). Acute Graft-versus-Host Disease-Biologic Process, Prevention, and Therapy. N. Engl. J. Med. 377, 2167–2179. [PubMed: 29171820]

Highlights

- Lysosomal acid lipase (LAL) is required for donor T cells to induce GVHD
- LAL regulates T cell immunity in GVHD target organs
- Pharmacological blockade of LAL effectively ameliorates GVHD
- Pharmacological blockade of LAL preserves GVL activity

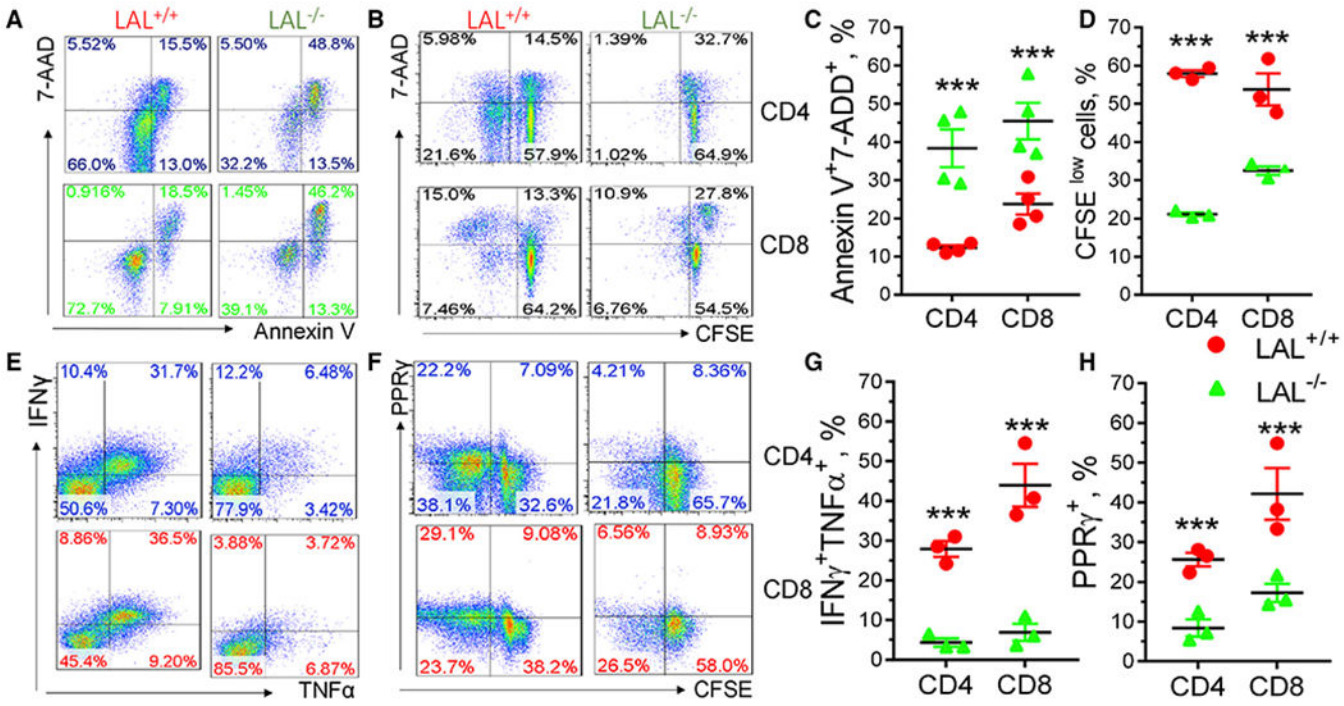

Figure 1. The Role of LAL in T Cell Survival, Proliferation, Cytokine Secretion, and Metabolism

CD25-depleted T cells, isolated from the spleens and lymph nodes of $LAL^{+/+}$ and $LAL^{-/-}$ age- and gender-matched mice, were labeled with CFSE and stimulated with plate-bound CD3 (2 μg/mL) and soluble CD28 (2 μg/mL) for 3 days. Cells were stained with fluorochrome anti-mouse CD4, CD8, live/death, annexin V, 7-AAD for surface or fixed/permeabilized followed by intracellular staining with IFN-γ, TNF-α, and PPR-γ. The zebra plots show flow staining of 7-AAD, annexin V (A), CFSE (B), TNF-α, IFN-γ (C), and PPR-γ (D) on CD4 and CD8 T cells. The summary graphs show the frequencies and numbers of T cell subsets (E).

The data were presented as means ± SDs of 3 technical replicates. ***$p < 0.001$.

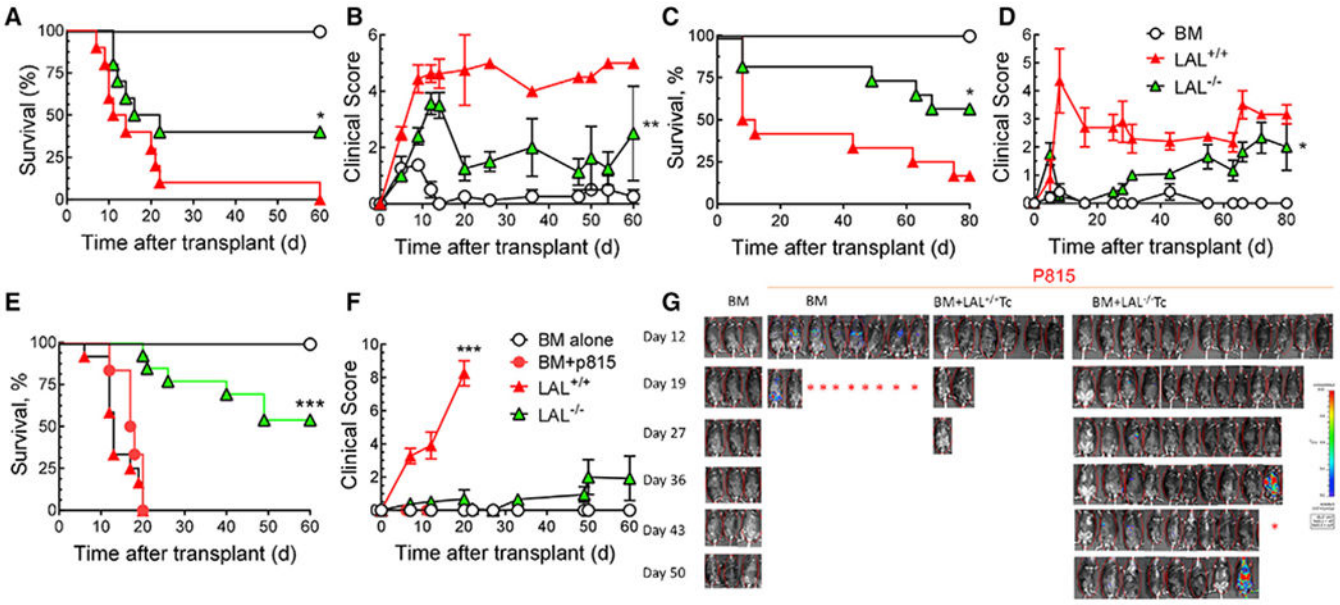

Figure 2. The Impact of LAL in Donor T Cells on GVHD and GVL Responses

(A and B) Lethally irradiated B6 recipients (n = 10–15) were transplanted with TCD-BM (5 × 10^6/mouse) from WT FVB mice without or with T cells (0.5 × 10^6/ mouse) from $LAL^{+/+}$ or $LAL^{-/-}$ FVB donors. The recipients were monitored for survival (A) and clinical scores (B).

(C and D) Lethally irradiated BALB/c recipients (n = 10) were transplanted with TCD-BM (5 × 10^6/mouse) from WT B6 without or with T cells (0.75 × 10^6/mouse) from $LAL^{+/+}$ or $LAL^{-/-}$ B6 donors. The recipients were monitored for survival (C) and clinical score (D).

(E–G) Lethally irradiated BDF1 recipients (n = 10) were injected with luciferase-transduced P815 mastocytoma (5,000 cells/mouse) and transplanted with TCD-BM (5 × 10^6/mouse) from WT B6 mice without or with CD25-depleted T cells (2.4 × 10^6/mouse) from $LAL^{+/+}$ or $LAL^{-/-}$ B6 donors. Survival (E), clinical score (F), and tumor signals reflected by bioluminescence intensity (G) are shown.

The log-rank (Mantel-Cox) test (A, C, and E) and nonparametric Mann-Whitney *U* test (B, D, and F) were used to compare between groups. The experiments were repeated 2 times. The data are presented as means ± SEMs; *p < 0.05, **p < 0.01, and ***p < 0.001.

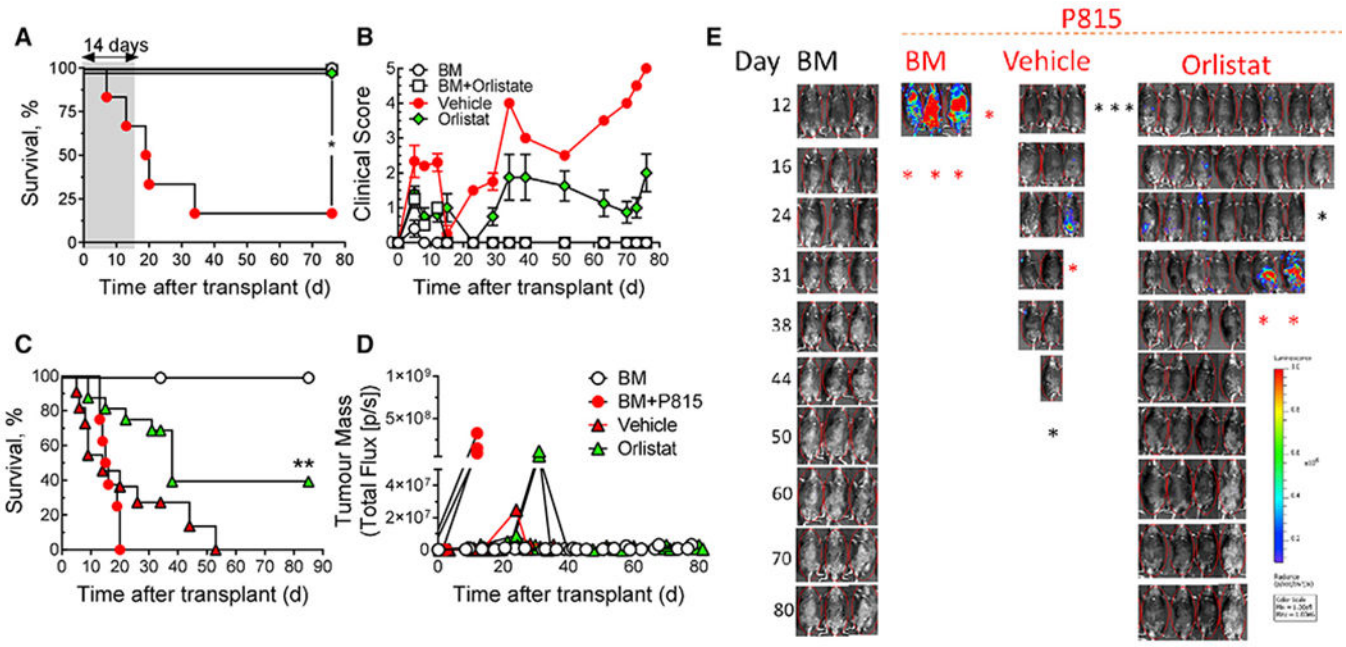

Figure 3. Pharmacological Inhibition of LAL with Orlistat Effects of GVHD and the GVL Effect

(A and B) Lethally irradiated BDF1 recipients (n = 10) were transplanted with TCD-BM (5 × 10^6/mouse) without or with CD25-depleted T cells (2.4 × 10^6/mouse) from B6 donors. Recipients were treated with orlistat intraperitoneally (i.p.) at 8 mg/kg every other day for 14 days. Recipient survival (A) and clinical scores (B) are shown.

(C–E) Allo-BMT was performed as in (A) and (B) (n = 10), except that recipients were injected with P815 mastocytoma (5,000 cells/mouse). Recipient survival (C), tumor signal (D), and summary of signal intensity (E) are shown.

The data are presented as means ± SDs; *p < 0.05 and **p < 0.01.

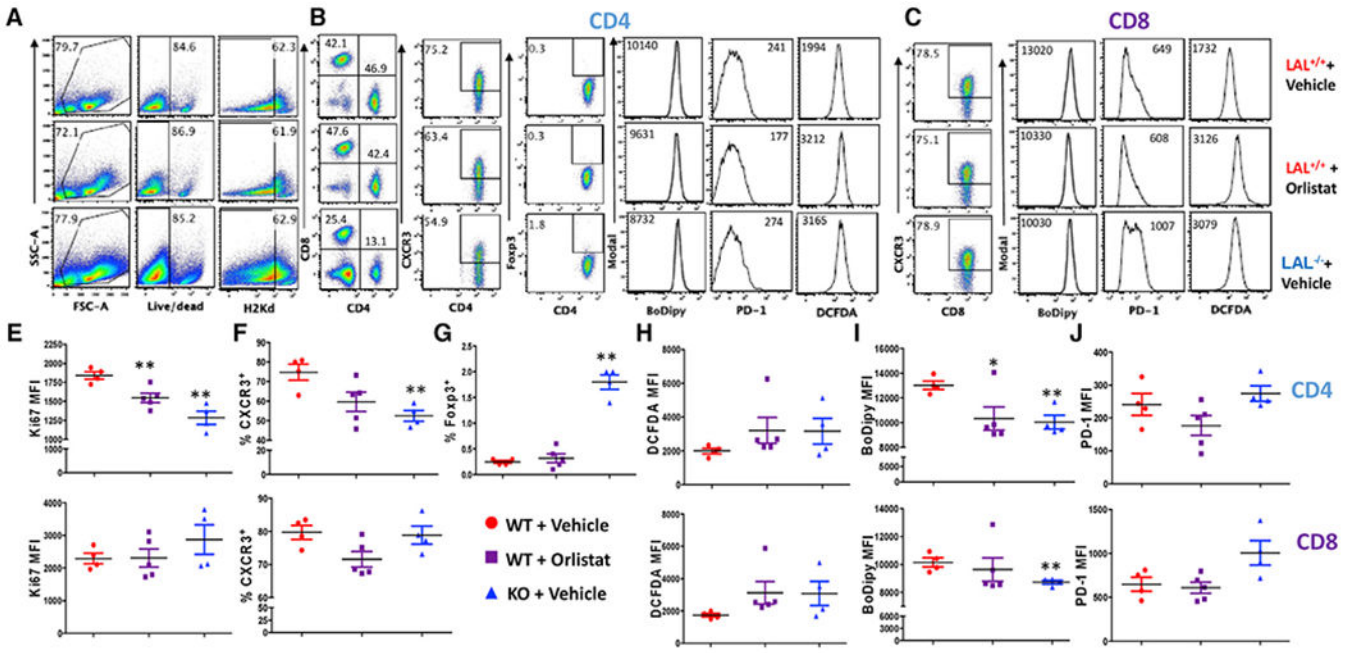

Figure 4. The Effect of LAL on T Cells in Recipient Spleen during GVHD

Lethally irradiated BDF1 recipients (n = 4–5) were transplanted with 5×10^6 $Rag^{-/-}$ BM cells and 1.25×10^6 CD25-depleted $LAL^{+/+}$ or $LAL^{-/-}$ T cells from B6 donors. Mice treated with orlistat received $LAL^{+/+}$ T cells and were i.p. injected with orlistat at a dose of 20 mg/kg/day. After 7 days, mice were euthanized, and their spleens were collected. Isolated cells from the spleens were stained and analyzed with flow cytometry.

(A-C) Cells were gated on live donor $CD4^+$ or $CD8^+$ cells (A) for downstream analysis. The frequency of $CXCR3^+$ or $CD4^+/Foxp3^+$, as well as the mean fluorescence intensity of BoDipy, PD-1, and DCFDA were measured for $CD4^+$ (B) or $CD8^+$ (C) cells.

(D–F) Summary graphs of the data.

The data are presented as means ± SEMs. The data shown are from 1 of 3 replicate experiments. *$p < 0.05$, **$p < 0.01$, and ***$p < 0.001$.

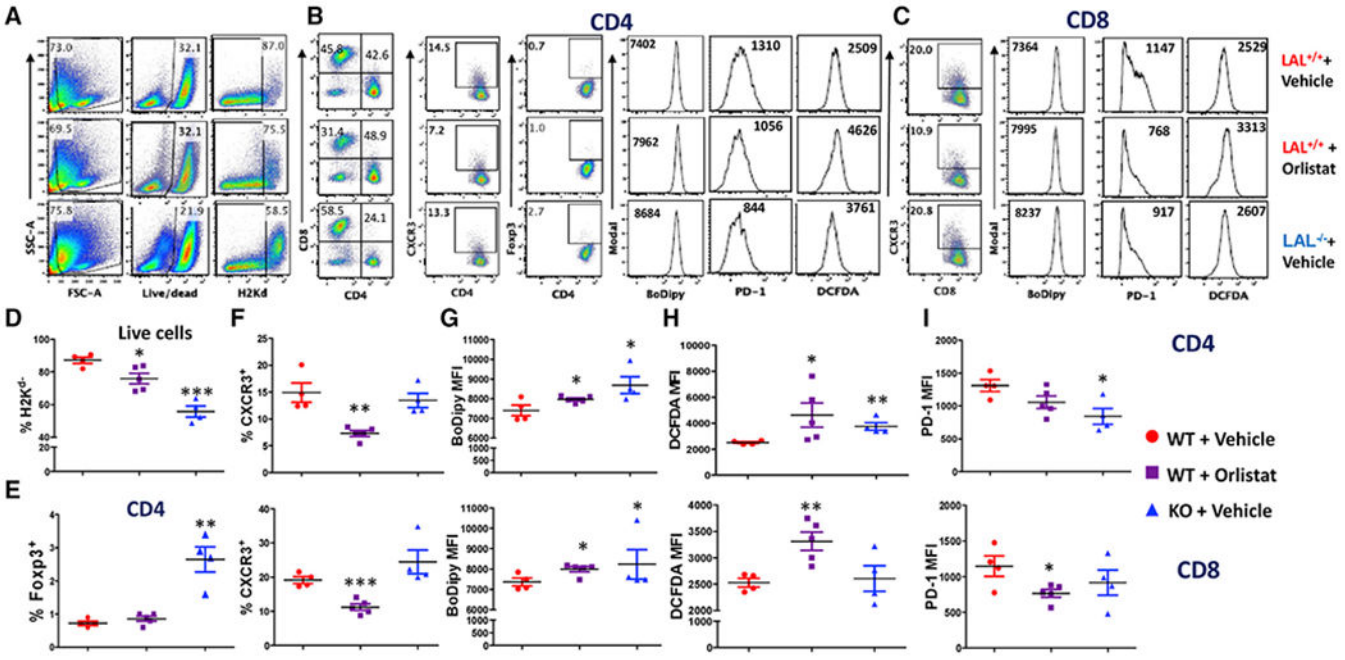

Figure 5. The Effect of LAL on T Cells in Recipient Intestines during GVHD

Allo-HCT was set up as described in Figure 4. After 7 days, mice were euthanized, and their intestines were collected. Isolated cells from the intestines were stained and analyzed with flow cytometry.

(A) Cells were gated on live donor $CD4^+$ or $CD8^+$ cells for downstream analysis.

(B and C) The frequency of $CXCR3^+$ or $CD4^+/Foxp3^+$, as well as the mean fluorescence intensity of BODIPY, PD-1, and DCFDA were measured for $CD4^+$ (B) and $CD8^+$ (C) cells.

(D–G) Summary graphs of the data.

The data are presented as means ± SEMs. The data shown are from 1 of 3 replicate experiments. *$p < 0.05$, **$p < 0.01$, and ***$p < 0.001$.

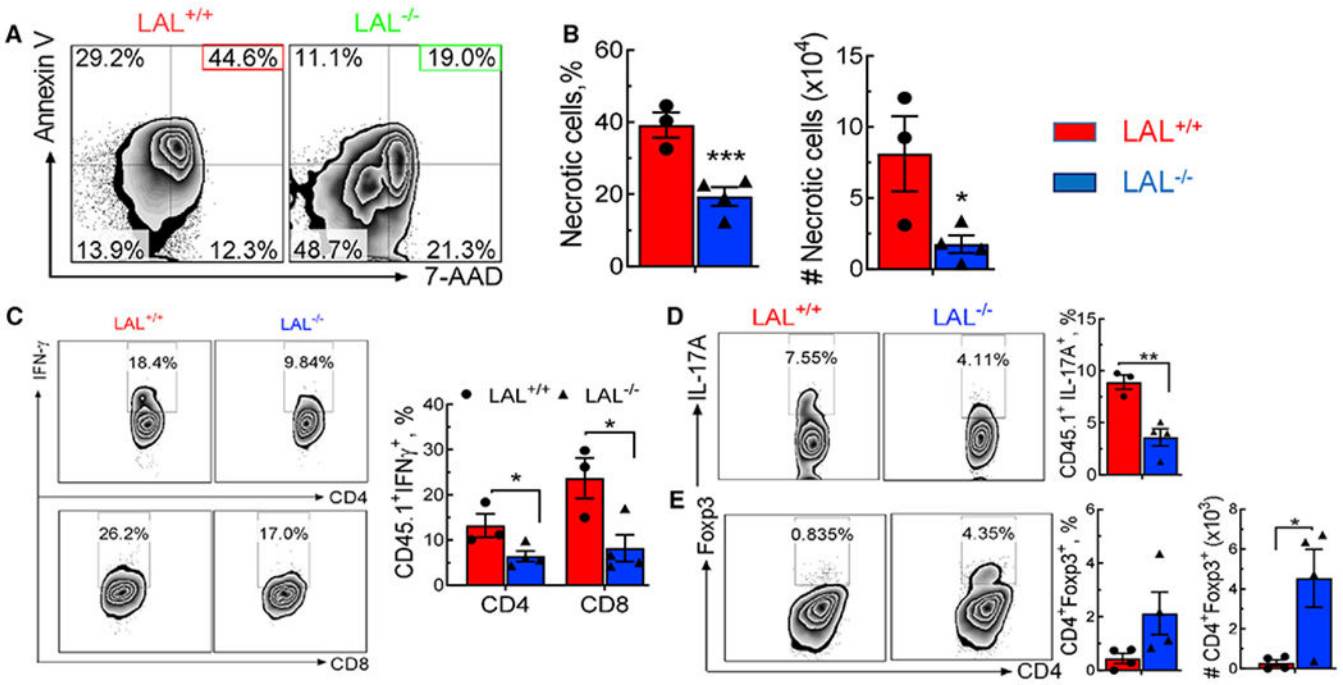

Figure 6. The Role of LAL in Donor T Cell Differentiation in the Gut

Lethally irradiated B6 recipients (n = 3–4) were transplanted with BM (5×10^6/mouse) from WT FVB mice without or with T cells (0.5×10^6/mouse) from $LAL^{+/+}$ or $LAL^{-/-}$ FVB donors. Thirteen days after transplant, the recipients were euthanized, and their spleens and intestines were collected. Isolated cells were stained for surface or intracellular makers by flow cytometry.

(A and B) The zebra plots (A) and summary graphs (B) show frequencies and numbers of recipient non-hematopoietic necrotic ($7\text{-AAD}^+\text{annexin V}^+$) cells isolated from the recipient guts.

(C–E) The zebra plots and summary graphs show frequencies of $IFN\gamma^+$ among donor CD4 or CD8 T cells (C), of $IL17A^+$ (D) and $Foxp3^+$(E) in donor CD4 T cells.

The Kruskal-Wallis test was used for statistical analysis. The experiments were repeated 2 times. The data are presented as means ± SDs from one representative experiment. *p < 0.05, **p < 0.01, and ***p < 0.001.

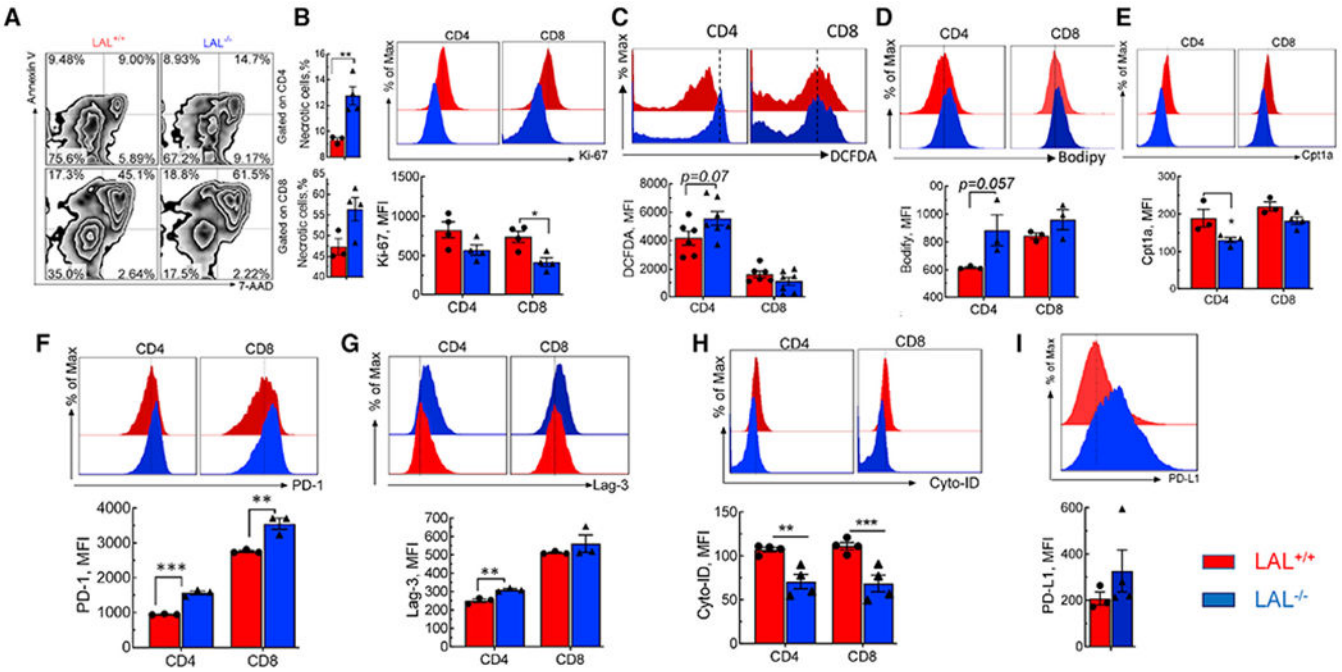

Figure 7. The Effect of LAL on T Cell Fate in Target Organs

Allo-HCT was set up and single cells were isolated on day 13 post-HCT and stained for analysis by flow cytometry, as in Figure 3.

(A) The zebra plots and summary graphs show the frequencies of donor necrotic (7-AAD$^+$ annexin V$^+$) on gated CD4 or CD8 T cells isolated from recipient guts.

(B–I) Histograms and summary graphs show mean of fluorescence intensity of Ki67 (B), DCFDA(C), BODIPY (D), cpt1a (E), PD-1 (F), lag-3 (G), and cyto-ID (H) and PD-L1 (I). The Kruskal-Wallis test was used for statistical analysis. The experiments were repeated 2 times. The data are presented as means ± SDs. *$p < 0.05$, **$p < 0.01$, and ***$p < 0.001$.

KEY RESOURCES TABLE

REAGENT or RESOURCE	SOURCE	IDENTIFIER
Antibodies		
Mouse anti-CD4	3D Biosciences	#560468 ; RRID:AB_1645271; Clone RM4-5
Mouse anti-CD8	3D Biosciences	#553035; RRID:N/A; Clone 53-6.7
Mouse anti-$H2^q$	BioLegend	#115106; RRID:AB_893562; Clone KH114
Mouse anti-CXCR3-biotin	Invitrogen	#13-1831-82; RRID:N/A; Clone CXCR3-173
Mouse anti-CCR6-AF647	Biolegend	#129808; RRID:AB_1877147; Clone 29-2L17
Mouse anti-FasL	BD Biosciences	#555293; RRID:N/A; Clone MFL3
Mouse anti-PD1	eBiosciences	#12-9985-81;RRID:N/A; Clone J43
Mouse anti-NK1.1	eBiosciences	#25-5941-81; RRID:N/A; Clone PK136
Mouse anti-CD44	Invitrogen	#12-0441-82; RRID:N/A; Clone IM7
Mouse anti-CD62L	Invitrogen	15-0621-82; RRID:N/A; Clone MEL-14
Mouse anti-TCRβ	BD Biosciences	#553171; RRID:N/A; Clone H57-597
Mouse anti-CD11b	eBiosciences	#13-0112-85; RRID:N/A; Clone M1/70
Anti-streptavidin-APCCy7	BD Biosciences	#554063; RRID:N/A
Anti-streptavidin-PECy7	BD Biosciences	#557598; RRID:N/A
Mouse anti-IFNγ	Invitrogen	#45-7311-82; RRID:N/A; Clone XMG1.2
Mouse anti-IL-17	Biolegend	#506922;RRID:AB_2125010; Clone TC11-18H10.1
Mouse anti-IL-4	BD Biosciences	#554435; RRID:N/A; Clone 11B11
Mouse anti-IL-5	Invitrogen	#12-7052-82; RRID:N/A; Clone TRFK5
Mouse anti-Foxp3	eBiosciences	#35-5773-82; RRID:N/A; Clone FJK-16 s
Mouse anti-Ki67	Biolegend	#652404; RRID:N/A; Clone 16A8
Mouse anti-pS6-AF467	Cell Signaling Technology	#4851S; RRID:AB_10695457; Clone D57.2.2E
CFSE	BD Biosciences	#565082; RRID:AB_2869649
Mouse anti-CD45R-biotin	Invitrogen	#13-0452-85; RRID:N/A; Clone RA3-6B2
Mouse anti-CD11b-biotin	Invitrogen	#13-0112-85; RRID:N/A; Clone M1/70
Mouse anti-TER-119-biotin	Invitrogen	#13-5921-85; RRID:N/A; Clone TER-119
Mouse anti-CD49b-biotin	Invitrogen	#13-5971-85; RRID:N/A; Clone DX5
Mouse anti-CD25-biotin	Invitrogen	#13-0251-85; RRID:N/A; Clone PC61.5
Mouse anti-CD90.2-biotin	BD Biosciences	#13-0903-81; RRID:N/A; Clone 30-H12
MitoTrackerRed	Invitrogen	#V35116; RRID:N/A
Mouse anti-Cpt1a	Abcam	#171449; RRID:N/A
2′,7’-Dichlorofluorescin diacetate	Sigma Aldrich	#4091-99-0; RRID:N/A
Bodipy	Invitrogen	#D-3823; RRID:N/A
Chemicals, Peptides, and Recombinant Proteins		
Rabbit complement	Immucor	RC-100
Cell-Tak	BD Biosciences	354240
Anti-biotin microbeads	Miltenyi Biotec	#130-090-485

REAGENT or RESOURCE	SOURCE	IDENTIFIER
Fetal bovine serum, charcoal-stripped	Thermo Fischer	#A3382101
N-acetyl-L-cysteine	Sigma-Aldrich	#A7250
Orlistat	Cayman Chemical Company	#10005426
Critical Commercial Assays		
Live dead yellow staining kit	Invitrogen	L-24968
Annexin V kit	BD Biosciences	#559763
Seahorse XF Glycolysis Stress Test Kit	Agilent	#103020-100
Seahorse XF Mito Stress Test Kit	Agilent	#103015-100
Experimental Models: Cell Lines		
Mouse: luciferase-transduced P815 mastocytoma	Dr. Pavan Reddy lab	N/A
Mouse: MLL-AF9 GFP^+ mixed lineage leukemia	Dr. Sophie Paczesny lab	N/A
Experimental Models: Organisms/Strains		
Mouse: C57BL/6 $LAL^{+/+/-/-}$	Original mice provided by Dr. Cong Yan lab; mice bred at MUSC	N/A
Mouse: FVB $LAL^{+/+/-/-}$	Original mice provided by Dr. Cong Yan lab; mice bred at MUSC	N/A
Mouse: BALB/c	NCI or Charles River	028
Mouse: FVB	NCI or Charles River	207
Mouse: C57BL/6	NCI or Charles River	027
Mouse: C57BL/6 $Ly5.1^+$	NCI or Charles River	494
Mouse: B6D2F1	NCI or Charles River	099
Mouse: C3H-SW	NCI or Charles River	N/A
Other		
Seahorse XFe96 Analyzer	MUSC Bioenergetics Profiling Core	#101991-100